Dissipative Double-Well Potential for Cold Atoms: Kramers Rate and Stochastic Resonance

Ion Stroescu,* David B. Hume,† and Markus K. Oberthaler
Kirchhoff-Institute for Physics, University of Heidelberg, INF 227, 69120 Heidelberg, Germany
(Received 23 February 2016; published 9 December 2016)

We experimentally study particle exchange in a dissipative double-well potential using laser-cooled atoms in a hybrid trap. We measure the particle hopping rate as a function of barrier height, temperature, and atom number. Single-particle resolution allows us to measure rates over more than 4 orders of magnitude and distinguish the effects of loss and hopping. Deviations from the Arrhenius-law scaling at high barrier heights occur due to cold collisions between atoms within a well. By driving the system periodically, we characterize the phenomenon of stochastic resonance in the system response.

DOI: 10.1103/PhysRevLett.117.243005

A classical particle confined in a dissipative double-well potential is a simple conceptual model that has, nonetheless, proved to be a powerful theoretical and experimental tool. In physical chemistry, for example, this model serves as the basis for much of reaction rate theory, as exemplified by the Kramers rate [1–4]. Here, a few basic parameters including the barrier height, the particle temperature, and the relevant trapping frequencies in one dimension are sufficient to understand the thermally driven transition rate. The same double-well model is the starting point for the theory of stochastic resonance, in which a system subject to a weak driving field exhibits a peak in its response as a function of the temperature [5].

Beyond its interest as a model system, a system of particles in a double-well potential can be a useful experimental tool. A particle in either well occupies a metastable state, and transitions between those states are driven by rare energetic processes. Whereas an ensemble measurement of an observable such as, for example, kinetic energy, will include only a negligible contribution from these rare events, an experiment that detects hopping events across a barrier is sensitive only to the high-energy tail of the energy distribution. This provides a background-free window into rare events that, nonetheless, dominate particle dynamics on longer time scales. Given suitable control and site-resolved particle detection, one can study these processes as a function of experimental parameters such as barrier height, temperature, and particle density. Such a systematic study can reveal the origin of these energetic processes and is essential for understanding the dynamics of the trapped particles.

Here, we realize a dissipative double-well system of cold trapped atoms and study the particle exchange rates and their underlying mechanisms over a range of experimental parameters. We produce the double-well potential by superimposing a magneto-optical trap (MOT) with a blue-detuned sheet of light. The latter is produced by a Gaussian laser beam with a large aspect ratio ($6 \times 400\ \mu\mathrm{m}^2$), creating a near uniform potential barrier through the MOT volume ($r_{\mathrm{MOT}} \sim 35\,\mu\mathrm{m}$). Under the effect of this barrier, one can observe a split MOT with the two sides separated by a sharp boundary limited by the optical resolution of the imaging system [Fig. 1(a)]. We can precisely control the barrier height ΔV by varying the power in the light sheet. In our system, laser cooling and heating provide dissipation in a way that allows for control of the temperature T. Furthermore, the particle number can be varied and precisely detected from the level of a single atom to thousands. We use this control to study particle exchange rates in different regimes dominated by both thermal and collisional processes.

The number of atoms N_1 and N_2 in each corresponding site is determined via fluorescence imaging. The scattered photons are collected in an imaging system with a numerical aperture of 0.23 and imaged onto a low-noise CCD camera. We have previously established a noise model for atom counting, taking into account the contributions of photon shot noise, fluorescence noise, and noise due to atom loss [6,7] and found a single-atom resolution limit for determining the atom number imbalance $z = (N_1 - N_2)/(N_1 + N_2)$ at a total of 500 particles.

We use two different methods to measure the hopping rates depending on the number of atoms. For mesoscopic atom numbers, an initial imbalance $z_0 \sim \pm 1$ is prepared, and the hopping rate r is deduced from the initial population increase of the empty site given by $\dot{N}_{1,2} = rN_{2,1}$. An example of this is shown in Fig. 1(b). After some time, the atom number imbalance equilibrates, while the total atom number $N = N_1 + N_2$ decreases due to the slower trap loss. If there are relatively few atoms in the trap, the hopping rate can be measured by detecting the individual anticorrelated jumps in the fluorescence signal over time corresponding to an atom leaving one well and entering the other. Here we obtain $r = \lambda/\langle N \rangle t$, where λ is the number of hopping events during the time t, and $\langle N \rangle$ is the time average of the total atom number. Example time traces shown in Fig. 1(c) illustrate how the dynamics slow down with increasing

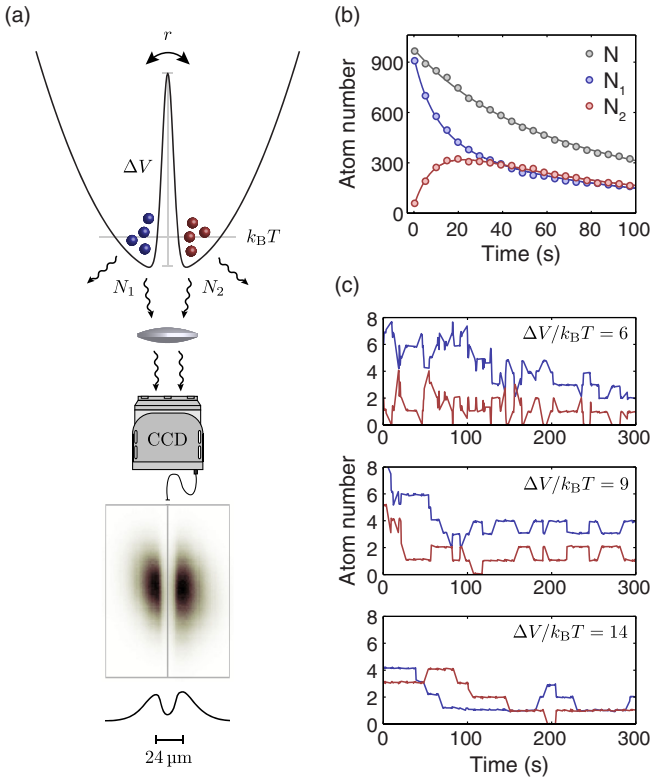

FIG. 1. Hybrid optical trap and hopping rate measurements. (a) The hopping rate r between the two sites of the dissipative double-well potential depends on both the potential barrier height ΔV and the temperature T. Fluorescence imaging with single-atom resolution yields the individual atom number N_1 and N_2. (b) An initial atom number imbalance equilibrates over time. For large atom numbers, the initial slope is a measure for the rate of light-assisted collisions. (c) Single-atom resolution allows the precise identification of hopping events as the anticorrelated atom number changes. Increasing the barrier height for a given temperature reduces the hopping rate.

potential barrier height. This method of measuring the hopping rate is sensitive for very low rates, where a long detection time is favorable. With an exposure time of 500 ms, we achieve a resolution as low as one event in 10^4 s, where we are ultimately limited by the feasible observation period.

While the dependence of the rate on ΔV is well described by Arrhenius's law, we see strong deviations from this model at larger barrier heights. The simple Arrhenius rate is obtained from a Gaussian velocity distribution $\mathcal{T}(v) = \sqrt{m/2\pi k_B T}\exp(-mv^2/2k_BT)$ for the thermal atomic sample, where T is the temperature, m is the mass, and k_B is the Boltzmann constant. However, the presence of light-assisted collisions will modify the wings of this distribution at a level dependent on the number of trapped atoms in each well. The energy gained by the process of light-assisted collisions is exponentially distributed, which can be modeled by $\mathcal{C}(E) = E_0^{-1}\exp(-E/E_0)$ with an energy scale E_0 depending on the detuning of the light [8,9]. In our experiment, $E_0/k_B = 3$ mK describes dependence of the hopping rate due to light-assisted collisions on the potential barrier height for mean atom numbers of 2500 and 320 shown in Fig. 2. $\mathcal{C}(E)$ can be expressed as a velocity distribution $\mathcal{C}(v)$ via $E = mv^2/2$, such that the combined velocity distribution $f(v) = (1-\varepsilon N)\mathcal{T}(v) + \varepsilon N\mathcal{C}(v)$ with $\varepsilon = 1.2(1)\times 10^{-7}$ describes the hopping rate measurements for large atom numbers N over the entire range of barrier heights. Taking the example of $N = 320$, although the fraction of atoms in the higher-energy component is only $\varepsilon N = 3.8(1)\times 10^{-5}$, this component dominates the hopping rate above a barrier height of $\Delta V \sim 10k_BT_0$, because the thermal hopping is sufficiently suppressed.

For small atom numbers, we measure a hopping rate at large barrier heights that is several orders of magnitude higher than the thermal hopping rate and at least 1 order of magnitude higher than the rate expected due to light-assisted collisions. Furthermore, since we observe no correlated loss events (i.e., events where two atoms are lost simultaneously) at these barrier heights, we can reject cold collisions as a cause of the observed loss. In general, the increased hopping rate may be described by a further modification of the thermal velocity distribution in addition to the modification due to light-assisted collisions, an anomalous diffusion rather than a Gaussian spatial diffusion [10–16]. We have investigated other possible sources of the observed hopping rate for small atom numbers, including quantum tunneling and effects from an inhomogeneous potential barrier and find them to be insufficient to

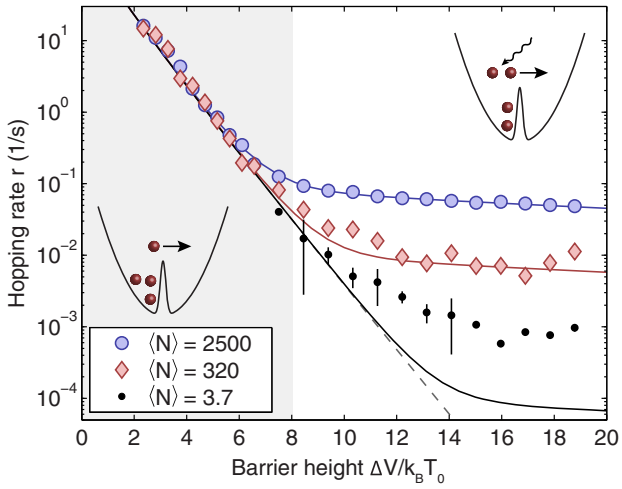

FIG. 2. The hopping rate dependence on small barrier heights is given by the Kramers rate (dashed line). At large enough barrier heights, the thermal activation is suppressed, and collisionally activated hopping starts to dominate for large mean atom numbers, such as 2500 (blue circles) and 320 (red diamonds). Including the high-energy scale of light-assisted collisions in the velocity distribution describes the scaling with atom number (solid lines). For small atom numbers, however, the measured hopping rate (black dots) is significantly higher than expected from light-assisted collisions.

account for our observation. Another source of this high-energy tail in the distribution could be collisions with background gas [17–19]. We measure an atom loss rate from background gas collision of $1/(250\ \mathrm{s})$. Our measured hopping rate can be explained if we assume a fraction of approximately $1/5$ of the background collision events leading to hopping rather than loss [20–29].

By adjusting the barrier height ΔV and temperature T, we can operate in a regime where particle exchange is dominated by thermal activation [20]. We have calibrated the steady-state MOT temperature with a release-and-recapture technique to be $T_0 = 80\ \mu\mathrm{K}$. The temperature of the atomic ensemble can be increased by switching to a blue detuning of $+\Gamma$, effectively heating the sample for a short period of time compared to the cooling of the atoms [see Fig. 3(a)]. The duty cycle d of blue detuning is given by $d = \tau_b/(\tau_b + \tau_r)$, where τ_b (τ_r) is the time of blue (red) detuning. We find $T(d) = T_0(1 - \xi d)^{-1}$, with $\xi = 3.6(1)$, which allows for a maximum duty cycle of about 27%. We explore the temperature dependence of the hopping rate for an intermediate barrier height, i.e., in the thermal hopping regime. Figure 3(b) shows an Arrhenius plot of $\log(r)$ against the inverse temperature, confirming the exponential scaling law in the hopping rate over 4 orders of magnitude.

This control over T and ΔV allows us to study the phenomenon of stochastic resonance, whereby a weakly

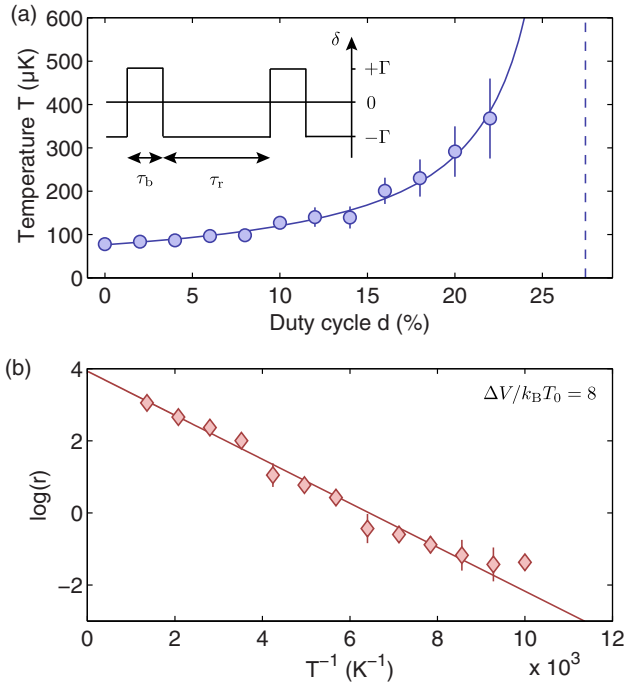

FIG. 3. Temperature control and Arrhenius's law. (a) The temperature of the laser-cooled atomic ensemble can be varied via the duty cycle of blue detuning, which can reach a maximum of 27% (dashed line). (b) An Arrhenius plot of $\log(r)$ versus the inverse temperature shows the expected linear dependence over 4 orders of magnitude.

driven system exhibits a maximum in its linear response as a function of the temperature. Given an external modulation of the system, the temperature can be tuned to match the hopping rate r to the modulation frequency $\Omega = 2\pi/T_\Omega$, where T_Ω is the modulation period. A harmonic modulation of the magnetic offset field of the MOT causes an imbalance in the population of the two sites illustrated in Fig. 4(a), which can be measured via the atom number imbalance z. The linear system response to the modulation can be written as $\langle x(t)\rangle = \bar{x}\cos(\Omega t - \phi)$, where $\bar{x}$ is the amplitude and ϕ the phase. When the time-scale matching condition $2/r = T_\Omega$, or, equivalently, $\Omega = \pi r$ is met, the amplitude of the linear system response exhibits a maximum. This implies that added (thermal) noise can *increase* the signal-to-noise ratio of an extracted signal [5].

The system response to a modulation of the harmonic MOT potential is observed in the normalized atom number difference z. We perform a nonuniform discrete Fourier transform $z(t) \to \tilde{z}(\nu)$ and obtain the power spectral density $P(\nu) \propto |\tilde{z}(\nu)|^2$ [20]. The peak strength of the frequency component equal to the driving frequency $\Omega = 2\pi\nu_0$ in the linear response theory is given by $P(\nu_0) = (\pi/2)\bar{x}^2(T) + P_N(\nu_0)$, where $P_N(\nu)$ the background power spectral density, i.e., the noise in the system response in the absence of driving. From this, we obtain the amplitude of the linear response $\bar{x}(T) = A_0\langle x^2\rangle_0/k_BT \times 2r_K/\sqrt{4r_K^2 + \Omega^2}$, where A_0 is the driving amplitude and $\langle x^2\rangle_0$ is the variance of the unmodulated system ($A_0 = 0$) [5]. The resonance shape of $\bar{x}(T)$ is shown in Fig. 4(b).

The stochastic resonance effect can be interpreted as tuning the noise level in order to obtain a maximum of the signal-to-noise ratio, which can be defined as $\mathrm{SNR} = 2P(\nu_0)/P_N(\nu_0)$. The factor of 2 reflects the property $P(\nu) = P(-\nu)$. In leading order, the signal-to-noise ratio can be expressed as $\mathrm{SNR} = \pi r_K(A_0x_0/k_BT)^2$, independent of the driving frequency Ω [30–32]. Like the linear response amplitude, the signal-to-noise ratio exhibits a maximum as a function of the system temperature shown in Fig. 4(b). Although the peak of both measures occur at similar temperatures, they do not necessarily coincide.

The phase of the linear response is given by $\phi(T) = \arctan(\Omega/2r_K)$ and vanishes for large noise intensities [33]. We confirm this by comparing the observed response phase with the driving phase given by the magnetic offset field modulation [see Fig. 4(b)]. In this higher-energy regime, the atoms move over the barrier at a rate much higher than the drive frequency. For lower temperatures, the response phase saturates to an expected value of $\pi/2$.

If we extract the linear response from the centroid of the atomic ensemble $c = \sum_i x_i/N$, rather than the atom number imbalance z, we become sensitive to the intrawell response of the atoms to the driving force [20,34,35]. This is caused by a shift $\delta x_m = x_m - x'_m$ between the unperturbed potential minimum x_m and the minimum x'_m altered by the driving [see the inset of Fig. 4(c)]. In this case, the response phase is

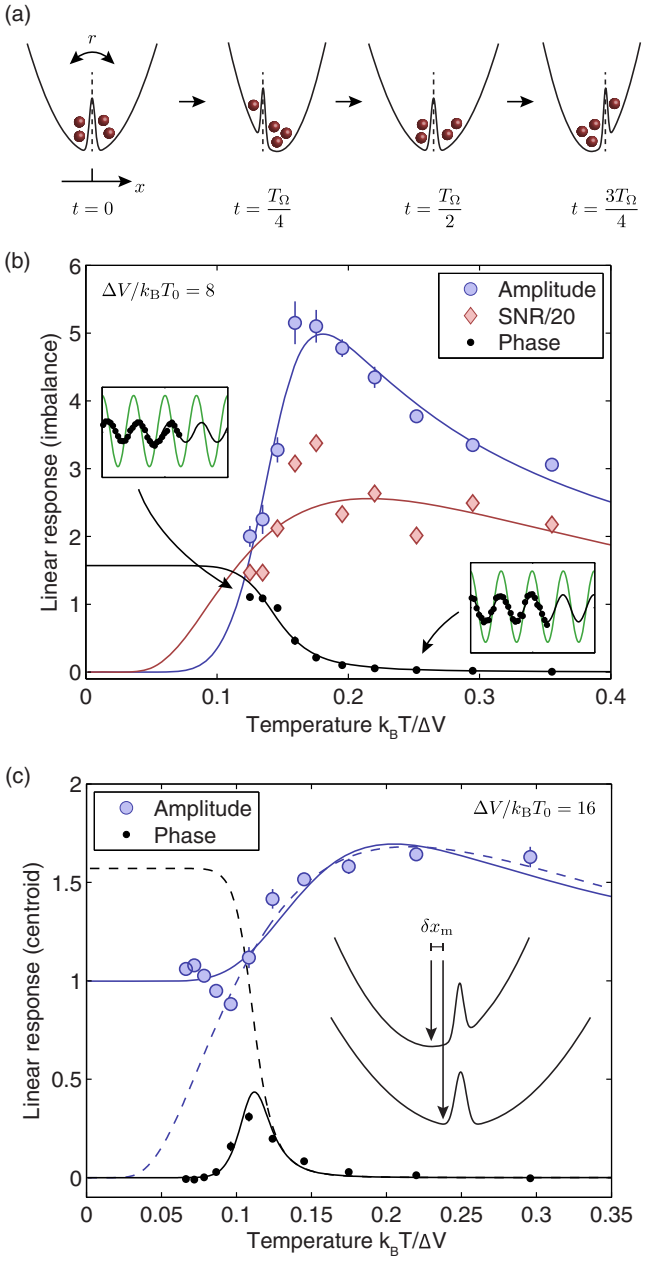

FIG. 4. Stochastic resonance. (a) The hopping rate r can be tuned via the temperature to match the time scale $T_\Omega = 2\pi/\Omega$ of the external modulation of the system, resulting in a stochastic resonance. (b) The linear response of the system extracted from the atom number imbalance shows the resonance feature in the amplitude as well as in the signal-to-noise ratio. The solid lines are fitted varying the driving amplitude A_0. The phase of the linear response exhibits the expected shift for temperatures below the resonance and approaches $\pi/2$ for vanishing thermal noise. The insets show the linear response (black dots) relative to the drive (green line). (c) Increasing the barrier height effectively probes lower temperatures, where the effects of intrawell motion are observed (solid lines), causing a deviation from the simple stochastic resonance theory (dashed lines). Here, the linear response is obtained from the motion of the atomic centroid. Intrawell motion is induced by a shift $\delta x_m = x_m - x'_m$ in the potential minima.

given by $\phi(T) = \arctan(\Omega/\omega_0(2\omega_0^2 r_K + \Omega^2 D)/(4\omega_0 r_K^2 + \Omega^2 D)$, where $D \propto T$ is the noise intensity, and ω_0 is the MOT trapping frequency at the potential minimum [36]. The phase goes to $\phi = \arctan(\Omega/\omega_0)$ for $T \to 0$, independent of the hopping rate, and since ω_0 is much larger than the driving frequency, this constant value is very close to zero, as shown in Fig. 4(c). We also observe the effects of intrawell motion on the linear response amplitude, which, for $T \to 0$, reduces to a finite constant $\bar{x}(T) \propto A_0\langle x^2\rangle_0/\sqrt{\omega_0^2 + \Omega^2}$ [37].

In conclusion, we have observed thermal and collisional processes in a dissipative double-well system with a high degree of control over the relevant parameters. We have measured transition rates between the two wells dominated by at least three different processes. At low barrier heights, the activation can be well described by Arrhenius's law describing thermal exchange for all atom numbers. At large barrier heights, depending on the density of atoms in the trap, light-assisted collisions lead to a small population at significantly higher energies that can dominate the exchange rate. At the highest barrier heights and low atom numbers, a separate process has been shown to dominate, which we have attributed to collisions with background gas. Our understanding of these dynamics allows us to apply a set of parameters where we observe the phenomenon of stochastic resonance, for which the hybrid trap is a paradigm system. Both the typical resonance shape of the linear response amplitude and the phase are altered by the presence of intrawell motion. In the future, an extension of our system to a hybrid trap with multiple wells and individually adjustable barrier heights could be used to study multidimensional energy transport in a controlled dissipative system, which is difficult to calculate theoretically, but experimentally accessible as an extension of the double-well potential to a hybrid optical lattice. We note also that our system of cold atoms confined to two wells separated by a controllable barrier realizes the setup of a classic Maxwell's demon gedanken experiment [38]. Further improvement of the atom imaging efficiency may allow for a direct realization of this and other foundational experiments.

We are grateful to P. Hänggi, W. Muessel, H. Strobel, and S. Jochim for discussions stimulating this work. We acknowledge financial support through the DFG Forschergruppe 760 "Scattering Systems with Complex Dynamics" of the Deutsche Forschungsgemeinschaft, the Heidelberg Center for Quantum Dynamics, and the European Commission FET-Proactive Grant AQuS (Project No. 640800). I. S. acknowledges support from the International Max Planck Research School (IMPRS-QD) and D. B. H. from the Alexander von Humboldt Foundation.

*dissipative@matterwave.de
†Present address: National Institute of Standards and Technology, 325 Broadway, Boulder, CO 80305, USA.

[1] H. A. Kramers, Physica (Utrecht) **7**, 284 (1940).
[2] K. J. Laidler and M. C. King, J. Phys. Chem. **87**, 2657 (1983).
[3] P. Hanggi, P. Talkner, and M. Borkovec, Rev. Mod. Phys. **62**, 251 (1990).
[4] E. Pollak and P. Talkner, Chaos **15**, 026116 (2005).
[5] L. Gammaitoni, P. Hanggi, P. Jung, and F. Marchesoni, Rev. Mod. Phys. **70**, 223 (1998).
[6] D. B. Hume, I. Stroescu, M. Joos, W. Muessel, H. Strobel, and M. K. Oberthaler, Phys. Rev. Lett. **111**, 253001 (2013).
[7] I. Stroescu, D. B. Hume, and M. K. Oberthaler, Phys. Rev. A **91**, 013412 (2015).
[8] P. S. Julienne and J. Vigué, Phys. Rev. A **44**, 4464 (1991).
[9] P. Sompet, A. V. Carpentier, Y. H. Fung, M. McGovern, and M. F. Andersen, Phys. Rev. A **88**, 051401 (2013).
[10] M. F. Shlesinger, G. M. Zaslavsky, and J. Klafter, Nature (London) **363**, 31 (1993).
[11] F. Bardou, J. P. Bouchaud, O. Emile, A. Aspect, and C. Cohen-Tannoudji, Phys. Rev. Lett. **72**, 203 (1994).
[12] S. Marksteiner, K. Ellinger, and P. Zoller, Phys. Rev. A **53**, 3409 (1996).
[13] H. Katori, S. Schlipf, and H. Walther, Phys. Rev. Lett. **79**, 2221 (1997).
[14] R. Metzler and J. Klafter, Phys. Rep. **339**, 1 (2000).
[15] Y. Sagi, M. Brook, I. Almog, and N. Davidson, Phys. Rev. Lett. **108** (2012).
[16] E. Lutz, Nat. Phys. **9**, 615 (2013).
[17] J. E. Bjorkholm, Phys. Rev. A **38**, 1599 (1988).
[18] S. Bali, K. M. O'Hara, M. E. Gehm, S. R. Granade, and J. E. Thomas, Phys. Rev. A **60**, R29 (1999).
[19] T. Arpornthip, C. A. Sackett, and K. J. Hughes, Phys. Rev. A **85**, 033420 (2012).
[20] See the Supplemental Material at http://link.aps.org/supplemental/10.1103/PhysRevLett.117.243005, which includes Refs. [21–29], for details on velocity distributions and hopping rates, nonuniform power spectral density, linear response amplitude and phase, as well as implications of intrawell motion.
[21] P. Jung and P. Hanggi, Europhys. Lett. **8**, 505 (1989).
[22] P. Jung and P. Hanggi, Phys. Rev. A **44**, 8032 (1991).
[23] B. McNamara, K. Wiesenfeld, and R. Roy, Phys. Rev. Lett. **60**, 2626 (1988).
[24] G. Debnath, T. Zhou, and F. Moss, Phys. Rev. A **39**, 4323 (1989).
[25] G. Vemuri and R. Roy, Phys. Rev. A **39**, 4668 (1989).
[26] T. Zhou and F. Moss, Phys. Rev. A **41**, 4255 (1990).
[27] M. I. Dykman, R. Mannella, P. V. E. McClintock, and N. G. Stocks, Phys. Rev. Lett. **65**, 2606 (1990).
[28] L. Gammaitoni and F. Marchesoni, Phys. Rev. Lett. **70**, 873 (1993).
[29] M. I. Dykman, R. Mannella, P. V. E. McClintock, and N. G. Stocks, Phys. Rev. Lett. **70**, 874 (1993).
[30] L. Gammaitoni, F. Marchesoni, E. Menichella-Saetta, and S. Santucci, Phys. Rev. Lett. **62**, 349 (1989).
[31] B. McNamara and K. Wiesenfeld, Phys. Rev. A **39**, 4854 (1989).
[32] C. Presilla, F. Marchesoni, and L. Gammaitoni, Phys. Rev. A **40**, 2105 (1989).
[33] L. Gammaitoni, F. Marchesoni, M. Martinelli, L. Pardi, and S. Santucci, Phys. Lett. A **158**, 449 (1991).
[34] G. Hu, H. Haken, and C. Z. Ning, Phys. Lett. A **172**, 21 (1992).
[35] P. Jung, Phys. Rep. **234**, 175 (1993).
[36] M. I. Dykman, R. Mannella, P. V. E. McClintock, and N. G. Stocks, Phys. Rev. Lett. **68**, 2985 (1992).
[37] P. Jung and P. Hanggi, Z. Phys. B **90**, 255 (1993).
[38] K. Maruyama, F. Nori, and V. Vedral, Rev. Mod. Phys. **81**, 1 (2009).